to be relatively close to that of tertiary amines (7.9 – 8.0 eV)[35] thus supporting the assignment of an ionization event out of a N lone pair. Bands ③ and ④ of the PE spectrum of **5a** are relatively close to those of the PE spectrum of **4a** which supports the assignment suggested in Figure 9.

Conclusive Remarks

Our model calculations combined with PE spectroscopic investigations reveal a consistent picture of the electronic structure of three-membered rings containing one to three phosphorus atoms. Due to the low symmetry of the species and the small energy separation between the basis orbital energies of the C–P, P–S, or P–N σ-bonds on one side and the lone pairs on P or the heteroatoms on the other, we encounter a strong mixing for most MO's. Due to this strong mixing the localization properties of the wave function of the HOMO depends on the substituents.

To illustrate this and to point out its consequence for the reactivity of phosphorus compounds, we mention the cage compounds **9** and **10**. While **9** reacts readily with transition-metal carbonyls like $Cr(CO)_6$ to yield $P_4[SiMe_2]_3{\cdot}Cr(CO)_5$ (**11**),[36] it is much more difficult to obtain a similar complex with **10**.[37] This difference has been rationalized by recognizing that the HOMO of **9** is a lone-pair combination localized at the basal three-membered ring while for **10** the HOMO is localized at the equatorial P atoms.[38]

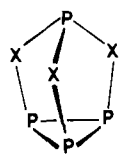

X = $Si(CH_3)_2$ **9**

X = PCH_3 **10**

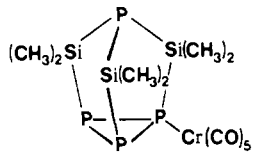

11

Experimental Section

The syntheses of compounds **1a**,[9] **4a**,[12] **5a**,[13] **6**,[14] and **7**[5] have been reported in the literature. The PE spectra were recorded on a UPS 200 spectrometer of Leybold Heraeus at the following temperatures: **1a**, 25 °C; **4a**, 45 °C; **5a**, 25 °C; **6**, 30 °C; and **7**, 50 °C. The spectra were calibrated with Ar and Xe.

Acknowledgment. We are grateful to the Deutsche Forschungsgemeinschaft, the Fonds der Chemischen Industrie, and the BASF Aktiengesellschaft, Ludwigshafen, for financial support. Thanks are due to A. Flatow for the PE measurements.

Registry No. **1a**, 99017-58-0; **1b**, 99017-51-3; **1c**, 6569-82-0; **2a**, 68969-73-3; *cis*-**2b**, 99017-57-9; *trans*-**2b**, 99017-52-4; *cis*-**2c**, 99017-56-8; *trans*-**2c**, 99017-53-5; **3a**, 61695-12-3; *cis*-**3b**, 99095-39-3; *trans*-**3b**, 91121-28-7; *cis*-**3c**, 99095-38-2; *trans*-**3c**, 89254-38-6; **4a**, 79898-83-2; **4b**, 99017-54-6; **4c**, 93109-87-6; **5a**, 82775-02-8; **5b**, 99017-55-7; **5c**, 77680-27-4; **6**, 77614-73-4; **7**, 76173-66-5.

(35) Aue, D. H.; Webb, H. M.; Bowers, M. T. *J. Am. Chem. Soc.* **1976**, *98*, 311.
(36) Fritz, G.; Uhlmann, R. *Z. Anorg. Allg. Chem.* **1980**, *465*, 59.
(37) Fritz, G.; Hoppe, K. D., private communication.
(38) Gleiter, R.; Böhm, M. C.; Eckert-Maksić, M.; Schäfer, W.; Baudler, M.; Aktalay, Y.; Fritz, G.; Hoppe, K. D. *Chem. Ber.* **1983**, *116*, 2972.

Kinetic Isotope Effect Associated with the Dissociative Addition of Dihydrogen to *trans*-$Ir(CO)Cl(Ph_3P)_2$[1a]

Peng Zhou,[†1b] Arturo A. Vitale,[†1c] Joseph San Filippo, Jr.,*[†] and William H. Saunders, Jr.*[‡]

Contribution from the Departments of Chemistry, Rutgers University, New Brunswick, New Jersey 08903, the University of Rochester, Rochester, New York 14627. *Received April 19, 1985*

Abstract: The temperature dependence of the kinetic isotope effect for the dissociative addition of dihydrogen and dideuterium to *trans*-$Ir(CO)(Cl)(Ph_3P)_2$ in toluene has been determined between 0 and 30 °C. Model calculations based on these data suggest that the transition state for dissociation is best formulated as triangular with reactant-like character and involves substantial hydrogen tunneling. The weak KIE ($k_H/k_D \approx 1$–2) generally observed for the dissociative addition of dihydrogen to transition-metal complexes is seen to be a consequence of the product of an unusually large MMI factor, a moderately inverse EXC term and a substantially inverse ZPE factor. Only the tunnel correction prevents the overall KIE from being inverse.

The addition of dihydrogen to a transition-metal center is an obligatory step in many catalytic cycles, and a variety of model systems have been investigated in an effort to understand the nature of such processes.[2] Of these, the addition of dihydrogen to *trans*-$Ir(CO)Cl(Ph_3P)_2$ (**1**) has been examined in greatest detail. Table I summarizes some of the previously determined kinetic parameters related to the addition of dihydrogen to **1**.[3-5]

Kinetic isotope effects afford a powerful technique with which to probe reaction mechanisms.[6] Despite this fact, there has been little effort to apply it to the dissociative addition of dihydrogen

(1) (a) Supported by the NSF, Grant CHE 83-12730. (b) Visiting Scholar, Institute for Applied Chemistry, Changchun, People's Republic of China. (c) Postdoctoral Fellow, Consejo Nacional de Investigaciones Cientificas y Technicas de la Republica Argentina.
(2) For a discussion, see: Collman, J. P.; Hegedus, L. "Principles and Applications of Organotransition Metal Chemistry;" University Science Books: Mill Valley, CA, 1980; p 187. James, B. R. "Homogeneous Hydrogenation"; Wiley: New York, 1973; pp 288–294. Lukehart, C. M. "Fundamentals of Transition Metal Organometallic Chemistry"; Brook/Cole: Belmont, CA, 1985; Chapter 10. Brown, J. M.; Parker, D. *Organometallics* **1982**, *1*, 950.
(3) Chock, P. B.; Halpern, J. *J. Am. Chem. Soc.* **1966**, *88*, 3511.
(4) (a) Strohmeier, W.; Onoda, T. *Z. Naturforsch.* **1968**, *23b*, 1377. (b) Strohmeier, W.; Onoda, T. *Ibid.* **1968**, *23b*, 1527. (c) Strohmeier, W.; Onoda, T. *Z. Naturforsch.* **1969**, *24b*, 515. (d) Strohmeier, W.; Muller, F. J. *Z. Naturforsch.* **1969**, *24b*, 770. (e) Strohmeier, W.; Muller, F. J. *Ibid.* **1969**, *24b*, 931. (f) Strohmeier, W.; Onoda, T. *Z. Naturforsch.* **1969**, *24b*, 1185.
(5) (a) Vaska, L.; Werneke, M. F. *Trans. N.Y. Acad. Sci.* **1971**, *31*, 70. (b) Vaska, L. *Acc. Chem. Res.* **1968**, *1*, 335.
(6) Cf.: Melander, L.; Saunders, W. H., Jr. "Reaction Rates of Isotopic Molecules"; Wiley: New York, 1980.

0002-7863/85/1507-8049$01.50/0

Table I. Kinetic Parameters Associated with the Addition of Hydrogen to *trans*-Ir(CO)(Cl)(PPh_3)$_2$

solvent	temp, °C	k_2, M^{-1} s^{-1}	ΔH^*, kcal/mol	ΔS^*, eu	exptl technique	ref
C_6H_6	20	0.50	10.8	−23	manometry	3
	25	0.67				
	30	0.93				
	35	1.30				
$C_6H_5CH_3$	20	0.31	10.7	−22	manometry	4
	25	0.44				
	30	0.59				
	20	0.34	*a*	*a*	manometry	3
	25	0.48	11	−22	spectrophotometry	5a
C_6H_5Cl	25	0.88	12	−20	spectrophotometry	5a
	30	1.2	11.5	−20	spectrophotometry	5b

[a] Not reported.

Table II. Kinetic Data for Addition of H_2 and D_2 to *trans*-IrCl(CO)(PPh_3)$_2$ in Toluene

temp, °C	k_H, M^{-1} s^{-1}	k_D, M^{-1} s^{-1}	activation parameters		k_H/k_D	A_H/A_D	$[\Delta E]^D_H$, kcal/mol
			E_H, kcal/mol	E_D, kcal/mol			
0.0	0.0832	0.0702	11.206 ± 0.066[c]	11.587 ± 0.048[c]	1.18_5	0.57	0.38
5.0	0.117	0.104			1.12_5		
			$A_H \times 10^{-8}$	$A_D \times 10^{-8}$			
10.0	0.173	0.155	0.774 ± 0.090[c]	1.35 ± 0.11[c]	1.11_6		
15.0	0.242	0.218			1.11_0		
			ΔH^*,[a] kcal/mol	ΔH^*,[a] kcal/mol			
20.0	0.341	0.311	10.634	11.015	1.09_6		
25.0	0.468	0.429			1.09_0		
			$-\Delta S^*_H$,[b] eu	$-\Delta S^*_D$,[b] eu			
30.0	0.634	0.595	24.35	23.24	1.06_5		

[a] Calculated with the equation $E_a = \Delta H^* + RT$; T = 288 K, the average temperature of the experiment. [b] Entropy of activation calculated with the expression $\Delta S^* = R(\ln A - \ln(kT/h) - 1)$, T = 288 K. [c] Standard deviation.

by transition-metal centers, and in those instances where KIE studies have been carried out, the results have been reported largely without interpretation or comment.[3,7]

The KIE associated with the addition of dihydrogen to transition-metal complexes is characterized by its unusual magnitude: the generally observed value is $k_H/k_D \approx 1$–2.[7] Weak primary isotope effects of this magnitude can arise in several ways, including (1) a limiting unsymmetry in the transition state, (2) heavy-atom participation in the reaction coordinate that results in an increase in the isotope-sensitive zero-point energy of the transition state, and/or (3) bending modes orthogonal to the reaction coordinate which add an additional isotope-sensitive zero-point energy to the transition state. We report here the results of a study which explains the curious kinetic isotope effect associated with the oxidative addition of dihydrogen to **1** and its significance in determining the nature of the dissociative addition of dihydrogen by many transition metals.

Results

Kinetics. Table II summarizes the kinetic parameters associated with the addition of dihydrogen and dideuterium to **1** in toluene. The diminished precision of earlier kinetic methodologies precluded the use of any of these techniques for determining the temperature dependence of the KIE associated with the dissociative addition of dihydrogen to **1**. The requisite precision was obtained by employing a differential capacitance monometer. The results are in generally good agreement with those determined with the lower-precision techniques outlined in Table I.

Model Calculations

Kinetic isotope effects can, in principle, reveal the nature and the timing of bonding changes during a reaction. Several methods are available for modeling kinetic isotope effects. The method we have employed, the so-called bond-order method, is based on the familiar concept of bond orders and employs them as independent variables in the modeling scheme. Other structural and bonding parameters required for the calculations are related to the bond orders by empirical or semiempirical relationships. An excellent review of bond-order methods for calculating kinetic isotpe effect has recently appeared.[8]

Table III. Bond Lengths and Force Constants Used in Calculations

bond length,[a] Å	stretching force constant,[b] mdyne/Å
Complex 1	
Ir–C 1.90	1.9
Ir–Cl 2.35	1.9
Ir–P 2.40	2.5
Complex 2	
Ir–H 1.60	2.79
Ir–C 1.90	1.9
Ir–Cl 2.35	1.9
Ir–P 2.40	2.5
H_2	
H–H 0.75	5.73

[a] Based on literature data (ref 20–31) on complexes **1** and **2**. Where bond lengths differ slightly, a compromise value is used. [b] From literature or estimated from literature frequencies (ref 20–31) and the equation $\omega = 1302.9\ (F/\mu)^{1/2}$, taking μ to be the reduced mass of Ir–X, where X = C, Cl, or P.

Bond lengths and vibrational frequencies for the reactant, **1**, and product, **2**, were used to estimate bond lengths and force constants for our models. These latter values are given in Table III.

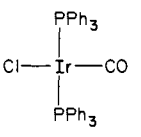

1

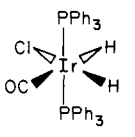

2

(7) Ozaki, A. "Isotopic Studies in Heterogeneous Catalysis"; Academic Press: New York, 1976; pp 172–178.

(8) Sims, L. B.; Lewis, D. E. In "Isotopes in Organic Chemistry;" Buncel, E., Lee, C. C., Eds.; Elsevier: Amsterdam, 1984; Vol. 6, pp 161–259.

Chart I. Linear (end-on) and Triangular (side-on) Transition States Proposed for Oxidative Addition of Dihydrogen to 1[a]

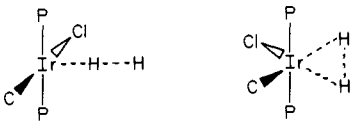

3A 3B

[a] Model 3A by itself does not account for the product-forming step. Its role is that of the rate-determining transition state which is followed by the formation of the second Ir-H bond.

Two rate-determining transition-state structures were selected for modeling, one involving a linear (end-on) coordination of hydrogen,[9] **3A**, and the other involving side-on coordination, **38**. Each structure is shown in Chart I in "proper" cutoff representation.[10,11] We considered **3A** to be a reactant-like transition state and consequently did not incorporate the geometric changes that must eventually occur as it is transformed into the product, **2**. Thus, H-H approaches Ir perpendicular to the plane defined by IrP$_2$CCl, and only the H-H and Ir-H bond orders change [n(Ir-H) = 1 - n(H-H)]. On the other hand, the ClIrCl angle is allowed to narrow as the IrH bonds form in **3B**, so as to approach the approximately octahedral geometry of the product **2**. Thus

$$\phi_{ClIrCl} = 90°[2 - n(Ir\text{-}H)]$$

Bond orders of 1.0 are assumed for the reactant H-H and D-D bonds. Similar standard bond orders apply to the product complex **2** and the reactant complex **1**. The bond orders of the transition-state models are primary parameters of the modeling scheme and are systemtically varied. These values are summarized in Table IV. We have assumed that bond order is conserved and, therefore, that the transition state is central and synchronous. The hybridization of Ir in the reactant complex **1** is dsp^2 (square planar) and in the transition states **3A** and **3B** ca. dsp^2 and ca. d^{2}sp^3 (octahedral), respectively. The nonreacting Ir-P, Ir-C, and Ir-Cl bonds suffer only small changes in bond length in going from reactant to product and, therefore, can be expected to undergo only correspondingly small changes in bond order and stretching force constants. These small changes in bond order and the accompanying changes in stretching force constants of the Ir-P, Ir-C, and Ir-Cl bonds can be neglected to a first approximation and retained at the reactant or product values.

The bond lengths r(H-H) and r(Ir-H) were adjusted by using Pauling's rule,[12,13] $r(n) = r(1) - 0.30 \ln (n)$, where $r(n)$ is the length of a bond of order n and $r(1)$ is the length of a single bond. Thus, the bond-order parameters of models **3A** and **3B** are the bond orders n(H-H) and n(Ir-H).

Geometric Considerations

Bond distances and angles as well as force constants of the reactant and transition-state models must be related to standard values and to assumed and/or assigned bond orders of the models by empirical and/or semiempirical relationships. Single bond lengths were used for all single bonds and the lengths of bonds of different order were adjusted from single bond values by Pauling's rule. The standard values employed were estimated from literature values and are given in Table III.

Internal Coordinates

The internal coordinates for both models were the various bond stretches and bond angle bends, including linear bands. This leads to five redundant coordinates for **3A**. In the case of **3B**, the H-Ir-H and the two H-H-Ir bends were omitted from the coordinate set so as to avoid problems associated with cyclic redundancies.[14] This leaves six redundancies arising from the hexacoordinate Ir.

Tunneling

Quantum mechanical tunneling becomes increasingly likely as the reaction barrier becomes more narrow and curved and as the effective mass decreases. Bell has proposed a correction for tunneling based on a one-dimensional barrier.[15] The first term of the Bell equation suffices for small-to-moderate tunnel corrections:

$$Q_t = (|u_L|/2)/\sin(|u_L|/2)$$

where $u_L = h|\nu_L^*|/kT$. Thus, the ratio Q_{tH}/Q_{tD} represents the factor which when multiplied by the semiclassical D-KIE, $(k_H/k_D)_s$, provides the tunnel-corrected value of k_H/k_D.

Reaction Coordinate Motion: Barrier Curvature Parameter. The reaction coordinate contribution to a kinetic isotope effect depends on the magnitude of the reaction coordinate frequency, ν_L^*, which according to transition-state theory can be either zero or imaginary. The reaction coordinate frequency as well as the real vibrational frequencies of the transition state result from solution of the vibrational secular equation

$$|\mathbf{GF} - \lambda\mathbf{E}| = 0$$

Upon removal of any redundant coordinates, matrix algebra assures that

$$\det \mathbf{GF} = \det \mathbf{G} \det \mathbf{F} = \prod_i \lambda_i$$

from which it follows that

$$\det \mathbf{F}_{TS} \leq 0$$

The off-diagonal elements of this determinant determine the coupled motions of H-H, Ir-H, etc., that allow the reaction system to become a TS. Inclusion of any number of pairs of coordinates (but usually adjacent bond stretches or a bond stretch and a bending of adjacent angles are coupled rather than coordinates involving atoms remote from one another) yields the equation

$$\det \mathbf{F}/\prod_i F_{ii} = P(A_{ij}) = D \leq 0$$

where D is referred to as the *barrier curvature parameter*. The exact form of the polynomial $P(A_{ij})$ must be derived by expansion of the determinant of the **F** matrix containing the desired interaction constants which, in turn, depends on the model under study.[6] For model **3A** the reacting bonds are

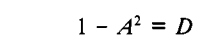

Letting

$$F_{12} = A(F_{11}F_{22})^{1/2}$$

gives

$$1 - A^2 = D$$

For model **3B** the reacting bonds are

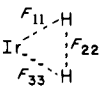

Letting

$$F_{12} = A(F_{11}F_{22})^{1/2} \qquad F_{23} = A(F_{22}F_{33})^{1/2}$$

gives

$$1 - 2A^2 = D$$

Calculation of KIE Values for Addition of Dihydrogen to 1

For each of the models **3A** and **3B**, n(Ir-H) was varied from reactant-like (0.1) to product-like (0.9) in steps of 0.2, with n-

(9) Ward, M. D.; Schwartz, J. *J. Mol. Catal.* **1981**, *11*, 397. Gell, K. I.; Schwartz, J. *J. Am. Chem. Soc.* **1978**, *100*, 3246. Ward, M. D.; Schwartz, J. *Organometallics* **1982**, *1*, 1030 and references therein.
(10) Wolfsberg, M.; Stern, M. J. *J. Pure Appl. Chem.* **1964**, *8*, 225-242.
(11) Stern, M. J.; Wolfsberg, M. *J. Chem. Phys.* **1966**, *45*, 4105-4124.
(12) Pauling, L. *J. Am. Chem. Soc.* **1947**, *69*, 542-553.
(13) Burton, G. W.; Sims, L. B.; Wilson, J. C.; Fry, A. *J. Am. Chem. Soc.* **1977**, *99*, 3371-3379.
(14) Keller, J. H.; Yankwich, P. E. *J. Am. Chem. Soc.* **1974**, *96*, 2303-2314.
(15) Bell, R. P. "The Tunnel Effect in Chemistry"; Chapman and Hall: New York, 1980;; pp 60-63.

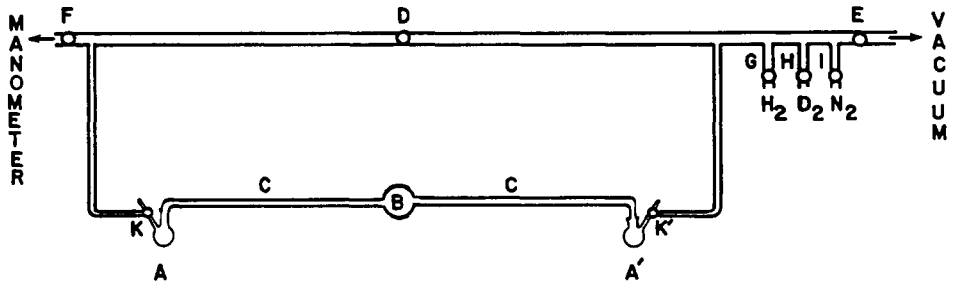

Figure 1. A schematic representation of the apparatus used to measure the absolute rate of reaction of *trans*-Ir(CO)Cl(Ph_3P)$_2$ with dihydrogen and dideuterium: A and A′ are 50-mL flasks (reaction and reference, respectively), each equipped with a Teflon-coated stirrer bar; B, is the differential Baratron; C, are connectors, vacuum jacket for temperature control; D, E, F, G, H, and I are 2-way vacuum stopcocks; K and K′ are three-way vacuum stopcocks.

Table IV. Bond Orders for Reactant, Product, and Transition-State Models for the Addition of Dihydrogen to **1**

	Bond Orders				
	reactants		transition state		product
bond	**1**	H_2	**3A**	**3B**	**2**
Ir–C	1.0		1.0	1.0	1.0
Ir–Cl	1.0		1.0	1.0	1.0
Ir–P	1.0		1.0	1.0	1.0
Ir–H	0.0		n(Ir–H)[a]	n(Ir–H)[a]	1.0
H–H		1.0	n(H–H)[a]	n(H–H)[a]	0.0

[a] The values of n(Ir–H) was varied from a low of 0.1 to a high of 0.9 in increments of 0.2. Similarly, the corresponding value of n(H–H) was incrementally varied between a maximum of 0.9 and a minimum of 0.1 so that n(H–H) = 1.0 − n(Ir–H).

(H–H) = 1 − n(Ir–H). Bond-stretching and bond-bending force constants involving these reacting bonds were varied according to the Pauling–Badger[16] relationship

$$F_R(n) = nF_R(1)$$

where $F_R(n)$ is the force constant for a bond of order n and $F_R(1)$ is the corresponding force constant for a single bond involving the same atoms. $F_R(1)$ values for stretching force constants in the complexes were estimated from literature frequencies and the equation

$$\nu\ (\text{cm}^{-1}) = 1302.9(F_R/\mu)^{1/2}$$

approximating the reduced mass as that for a diatomic molecule made up of the two atoms forming the bond (see Table III). There are almost no data on bending frequencies of the complexes, so all bending force constants, F_b, were arbitrarily assigned the same value in any given calculation, but this value was varied from 0.1 to 0.2 to 0.4 to 0.6 mdyn Å^{-1}/r_1r_2 so as to cover a range encompassing all likely values. Models employing a range of values of the curvature parameter D were included. The more negative the value of D, other factors being equal, the larger the tunnel correction.

The BEBOVIB-IV program of Sims, Burton, and Lewis was used for the calculations.[17] The most significant results are listed in Tables V–VII. A wider range of models was examined, but in no case did the omitted models give results even remotely compatible with the experimental values.

Results

The general expression for the KIE can be written as a product of four terms[6]

$$k_H/k_D = Q_{tH}/Q_{tD}\cdot\text{MMI}\cdot\text{EXC}\cdot\text{ZPE}$$

The first term is the tunnel correction, the second is the mass and moment-of-inertia term (arising from the translational and rotational partition functions), the third is the excitation term (arising from the vibrational partition functions), and the last is the zero-point-energy term. Representative results for model **3A** are given in Table V and for **3B** in Table VI. The factors contributing to the KIE for the model **3B** with A = 0.949 and F_b = 0.1 are given in Table VII.

Some general points can be made immediately. First, the MMI term is very large (ca. 5.5) for all trangular models and still rather large (ca. 2.4) for all linear models. This situation arises because isotopic substitution has a large effect on the MMI term for the reactant (H_2 vs. D_2) but a much smaller effect on the more massive transition state. Thus, other contributions less than unity are required for any model that will fit the unusually small observed KIE. While the EXC term runs below unity, the ZPE term is even smaller in most cases. But ZPE < 1 requires an *inverse* temperature dependence (KIE increasing with increasing temperature), contrary to experimental fact. Thus, a tunnel correction, which decreases with increasing temperature, is required to give the observed normal temperature dependence. The small observed KIE, consequently, can be seen to be the result of rather large but compensating contributions.

Closer examination of Table V shows that most of the linear models (**3A**) give isotope effects that are substantially larger than the experimental values. Only the model with A = 1.095 and F_b = 0.6 comes even close to reproducing the observed k_H/k_D values, but the inverse temperature dependence renders this model unacceptable. It is hard to conceive of any realistic variant of the linear model that would give acceptable KIE values. Some improvement might result from a larger A and a larger F_b, which could reduce $(k_H/k_D)_s$ and increase Q_{tH}/Q_{tD}, thereby leading to a more nearly normal temperature dependence. But F_b = 0.6 already makes the bending motions quite stiff, and much larger values of F_b seem quite unreasonable.

On the other hand, it is easier with the triangular model, **3B**, to obtain k_H/k_D values close to those observed and at the same time to match the observed temperature dependence. Table VI shows a number of variants of model **3B**, none of which fit the experimental results closely, but from which we selected the region A = 0.949–1.000, F_b = 0.1–0.2, and n(Ir–H) = 0.5–0.7 for further exploration. The two best models we found within this region are compared with experiment in Table VII. The first reproduces the temperature dependence very well, while the second reproduces the k_H/k_D values somewhat better than the first at the price of a poorer match on the temperature dependence. Further exploration of the parameter values would undoubtedly afford other good fits to experiment, but the essential characteristics of a successful model are already sufficiently apparent. Table VIII lits the components of the calculated k_H/k_D for the two best-fit models of Table VII. The essential role of tunneling in compensating for an inverse ZPE factor can readily be seen.

Experimental Section

General. Ambient and subambient temperature control to within 0.01 °C was achieved with a Lauda Ultra-Kryostat Model UK-50SDW.

trans-(Ph_3P)$_2$Ir(CO)Cl was prepared as described by Collman, Sears, and Kubota.[18a]

(16) Reference 6, p 185.

(17) Sims, L. B.; Burton, G.; Lewis, D. E., BEBOVIB-IV, Quantum Chemistry Program Exchange, Department of Chemistry, Indiana University, Bloomington, Indiana, 47401, Program No. 337.

(18) (a) Collman, J. P.; Sears, C. T.; Kubota, M. *Inorg. Synth.* **1968**, *11*, 101. (b) Cook, M. W. *J. Chem. Phys.* **1957**, *26*, 748.

Table V. Computed KIE and Arrhenius Parameters Associated with a Linear Transition State (Model **3A**)

			n(Ir–H) = 0.1				n(Ir–H) = 0.3				n(Ir–H) = 0.5			
A	F_b	temp, °C	$(k_H/k_D)_s$[a]	k_H/k_D[b]	A_H/A_D	$[\Delta E]_H^D$	$(k_H/k_D)_s$[a]	k_H/k_D[b]	A_H/A_D	$[\Delta E]_H^D$	$(k_H/k_D)_s$[a]	k_H/k_D[b]	A_H/A_D	$[\Delta E]_H^D$
1.0	0.4	0	1.530		1.92	−0.124	1.585		2.49	−0.246	2.011		2.71	−0.162
		17	1.553				1.631				2.051			
		34	1.571				1.669				2.082			
		50	1.585				1.700				2.106			
1.095	0.4	0	1.583	1.641	1.87	−0.070	1.662	1.921	2.16	−0.064	2.079	2.848	1.90	−0.218
		17	1.603	1.655			1.705	1.936			2.116	2.777		
		34	1.619	1.666			1.741	1.948			2.145	2.721		
		50	1.631	1.674			1.769	1.956			2.166	2.676		
1.095	0.6	0	1.309	1.358	2.06	−0.226	1.144	1.322	2.43	−0.329	1.322	1.810	2.13	−0.088
		17	1.350	1.393			1.208	1.371			1.390	1.824		
		34	1.384	1.424			1.265	1.415			1.450	1.840		
		50	1.412	1.448			1.313	1.452			1.502	1.856		

			n(Ir–H) = 0.7				n(Ir–H) = 0.9			
A	F_b	temp, °C	$(k_H/k_D)s$[a]	k_H/k_D[b]	A_H/A_D	$[\Delta E]_H^D$	$(k_H/k_D)_s$[a]	k_H/k_D[b]	A_H/A_D	$[\Delta E]_H^D$
1.0	0.4	0	2.800		2.71	0.018	3.324		2.52	0.151
		17	2.800				3.277			
		34	2.799				3.230			
		50	2.784				3.183			
1.095	0.4	0	2.800	4.638	1.40	0.650	3.324	4.322	1.92	0.441
		17	2.800	4.295			3.277	4.116		
		34	2.794	4.041			3.231	3.947		
		50	2.784	3.854			3.188	3.811		
1.095	0.6	0	1.738	2.879	1.53	0.340	2.084	2.710	2.04	0.154
		17	1.797	2.756			2.119	2.662		
		34	1.847	2.672			2.148	2.623		
		50	1.888	2.613			2.170	2.594		

[a] Semiclassical isotope effect (without tunneling). [b] Isotope effect with tunneling.

Table VI. Computed KIE and Arrhenius Parameters Associated with a Triangular Transition State (Model **3B**)

			n(Ir–H) = 0.1				n(Ir–H) = 0.3				n(IrH) v 0.5			
A	F_b	temp, °C	$(k_H/k_D)_s$[a]	k_H/k_D[b]	A_H/A_D	$[\Delta E]_H^D$	$(k_H/k_D)_s$[a]	k_H/k_D[b]	A_H/A_D	$[\Delta E]_H^D$	$(k_H/k_D)_s$[a]	k_H/k_D[b]	A_H/A_D	$[\Delta E]_H^D$
0.894	0.2	0	1.018	1.188	1.52	−0.134	0.639	0.969	1.43	−0.212	0.448	0.744	1.39	−0.38
		17	1.053	1.205			0.691	0.987			0.501	0.770		
		34	1.084	1.221			0.740	1.009			0.552	0.800		
		50	1.109	1.234			0.783	1.029			0.598	0.829		
0.949	0.1	0	1.049	1.299	1.37	−0.030	0.729	1.410	0.808	0.299	0.576	1.498	0.451	0.643
		17	1.080	1.302			0.778	1.347			0.628	1.353		
		34	1.108	1.306			0.822	1.313			0.677	1.282		
		50	1.131	1.310			0.860	1.295			0.720	1.247		
1.00	0.1	0	0.992	1.304	1.31	−0.003	0.603	1.481	0.510	0.572	0.414	1.536	0.181	1.14
		17	1.027	1.302			0.654	1.355			0.465	1.265		
		34	1.058	1.303			0.703	1.291			0.515	1.155		
		50	1.084	1.305			0.745	1.258			0.560	1.108		

			n(Ir–H) = 0.7				n(Ir–H) = 0.9			
A	F_b	temp, °C	$(k_H/k_D)_s$[a]	k_H/k_D[b]	A_H/A_D	$[\Delta E]_H^D$	$(k_H/k_D)_s$[a]	k_H/k_D	A_H/A_D	$[\Delta E]_H^D$
0.894	0.2	0	0.350	0.477	2.42	−0.881	0.210	0.210	2.99	−1.441
		17	0.401	0.524			0.246	0.246		
		34	0.451	0.570			0.282	0.282		
		50	0.498	0.613			0.316	0.316		
0.949	0.1	0	0.508	1.059	0.89	0.089	0.548	0.627	1.71	−0.508
		17	0.563	1.031			0.608	0.684		
		34	0.614	1.026			0.664	0.734		
		50	0.661	1.032			0.715	0.786		
1.00	0.1	0	0.320	0.716	0.935	−0.149	0.310	0.312	3.83	−1.359
		17	0.369	0.713			0.360	0.362		
		34	0.417	0.727			0.410	0.413		
		50	0.462	0.747			0.457	0.460		

[a,b] See corresponding footnotes to Table V.

Kinetic Measurements. The kinetics of the reaction of **1** with H_2 and D_2 were determined by measuring the change in pressure of each gas employing an MKS differential Baratron, Model 145 AH-1, with a range of 1.0000 mmHg. The initial concentration of **1** in these experiments ranged from 1.3×10^{-3} to 3.5×10^{-3} M. The initial partial pressure of each gas was ca. 760 mmHg, and their corresponding concentrations in solution were computed from solubility data in the literature.[18b] All kinetic runs were carried out at <5% conversion, making it possible to employ the method of initial rates.[19]

(19) (a) Moore, J. W.; Pearson, R. G. "Kinetics and Mechanism;" Wiley: New York, 1981, pp 67 and 68. (b) Stiger, H.; Kelm, H. *J. Phys. Chem.* **1973**, *77*, 290.

Table VII. Comparison of Experimental KIE with KIE Calculated from Model **3B**, $A = 0.975$, for the Reaction of **1** with H_2 and D_2

	k_H/k_D		
temp, °C	exptl	calcd[a,c]	calcd[b,c]
0	1.170	1.218	1.164
5	1.147	1.202	1.143
10	1.140	1.186	1.124
20	1.125	1.158	1.088
25	1.107	1.144	1.071
30	1.072	1.132	1.056
$E_D - E_H$	0.406 ± 0.063	0.401	0.534
A_H/A_D	0.554 ± 0.062	0.581	0.435

[a] $F_b = 0.1$; n(Ir-H) = 0.7. [b] $F_b = 0.2$; n(Ir-H) = 0.5. [c] Since the experiments and calculations did not employ identical sets of temepratures, these values are obtained from the Arrhenius parameters of the calculated values.

Table VIII. Summary of the Various Components of the Calculated KIE for the Reaction of **1** with H_2 and D_2 at 273 K, Transition State **3B**, $A = 0.949$

n(Ir-H)	F_b	MMI	EXC	ZPE	$(k_H/k_D)_s$	Q_{tH}/Q_{tD}	k_H/k_D
0.7	0.1	5.474	0.788	0.115	0.498	2.477	1.233
0.5	0.2	5.465	0.826	0.093	0.421	2.808	1.183

Figure 1 illustrates the experimental apparatus. In a typical run, 15.0 mL of a standard solution of **1** in toluene was injected by syringe into A. An equal amount of pure toluene was injected into A'. Each flask was equipped with a Teflon-coated stirring bar. A and A' were placed in a dry ice bath and subsequently evacuated to a pressure of 10^{-3} mmHg. The stopcock E was closed and each vessel allowed to warm to ambient temperature. This freeze-thaw cycle was repeated three additional times, at which point both flasks were submerged in a constant temperature bath and the contents of each flask stirred vigorously. After a period of time sufficient to reach thermal equilibrium (15-30 min), hydrogen (deuterium) was simultaneously admitted to A and A' until a pressure of ca. 760 mmHg was reached. The stopcocks K and K' were then closed and data collection commenced.

Digitalization of the rate data was achieved by interfacing the analogue signal output from the MKS Model 170M-26A pressure meter through a Tecmar Lab Master A/D converter and subsequently to an IBM XT computer with use of the ASYST software system purchased from Macmillan Publishing Co. Pressure readings were recorded at intervals of 0.500 s (25-30 °C), 1.000 s (0-20 °C) and 2.000 s (<0 °C).

Registry No. 1, 15318-31-7; H_2, 1333-74-0; D_2, 7782-39-0.

(20) Muir, K. W.; Ibers, J. A. *J. Organomet. Chem.* **1969**, *18*, 175.
(21) Chen, J.-Y.; Halpern, J.; Molin-Case, J. *J. Coord. Chem.* **1973**, *2*, 239.
(22) Khare, G.; Eisenberg, R. *Inorg. Chem.* **1972**, *11*, 1385.
(23) Bonnet, J.-J.; Jeannin, Y. *J. Inorg. Nucl. Chem.* **1973**, *35*, 4103.
(24) Bird, P.; Harrod, J. F.; Than, K. A. *J. Am. Chem. Soc.* **1974**, *96*, 1222.
(25) Shultz, A. J.; Khare, G.; McArdle, J. V.; Eisenberg, R. *J. Am. Chem. Soc.* **1973**, *95*, 3434.
(26) Stancel, J. R.; Wellington, P. *Acta Crystallogr., Sect. A* **1969**, *25*, 5172.
(27) Quiksall, C. O.; Spiro, T. G. *Inorg. Chem.* **1969**, *8*, 2011, 2363.
(28) Nakamoto, K. "Infrared Spectra of Inorganic and Coordination Compounds;" Wiley: New York, 1970; pp 204-206.
(29) Taylor, R. C.; Young, J. F.; Wilkinson, G. *Inorg. Chem.* **1966**, *5*, 20.
(30) Muetterties, E. L., Ed. "Transition Metal Hydrides;" Dekker: New York, 1971; Chapters 3 and 4.
(31) Adams, D. M. "Metal-Ligand and Related Vibrations"; St. Martins: New York, 1968; p 20.

Charge Carrier Trapping and Recombination Dynamics in Small Semiconductor Particles

Guido Rothenberger,[†] Jacques Moser,[†] Michael Grätzel,*[,†] Nick Serpone,[‡] and Devendra K. Sharma[‡]

Contribution from the Institut de Chimie Physique, Ecole Polytechnique Fédérale, CH-1015 Lausanne, Switzerland, and the Chemistry Department, Concordia University, Montréal, Québec, Canada. *Received July 31, 1985*

Abstract: By using picosecond or nanosecond laser photolysis to excite colloidal (diameter 120 Å) particles of TiO_2 in aqueous solution, we have monitored the dynamics of charge carrier trapping and recombination in this semiconductor and interpret the results by a stochastic kinetic model. While the absorption spectrum of the trapped electron appears within the leading edge of the 30-ps laser pulse, the trapping of the hole is a much slower process requiring on the average 250 ns. At high electron-hole pair concentration in the particles, their recombination follows a second order law, the rate coefficient being $(3.2 \pm 1.4) \times 10^{-11}$ cm^3 s^{-1}. Intraparticle recombination becomes first order at very low charge carrier occupancy, the lifetime of a single electron-hole pair in a 120 Å sized TiO_2 particle being (30 ± 15) ns. Under these conditions, hole trapping, presumably by surface hydroxyl groups, competes with recombination and leads to a product whose reaction with trapped electrons is relatively slow. Implications for charge carrier mediated photoreactions are discussed.

Methods have recently been developed to produce stable dispersions of colloidal semiconductors with narrow size distribution. Due to their ultrafine size, these particles form transparent solutions which are amenable to analysis by laser photolysis technique.[1] So far studies have concentrated on interfacial charge transfer between the semiconductor and solution species or catalysts deposited on the semiconductor surface.[2] A microwave technique has been used to probe electronic processes in small particle suspensions.[3] We apply here for the first time picosecond time-resolved spectroscopy to elucidate the dynamics of charge carrier reactions within the semiconductor particle. The systems studied are 120 Å sized TiO_2 particles in aqueous solution. Photoinduced, charge carrier related processes in TiO_2 play a key

[†] Institut de Chimie Physique.
[‡] Concordia University.

(1) (a) Duonghong, D.; Borgarello, E.; Grätzel, M. *J. Am. Chem. Soc.* **1981**, *103*, 4685. (b) Kalyanasundaram, K.; Borgarello, E.; Duonghong, D.; Grätzel, M. *Angew. Chem., Int. Ed. Engl.* **1981**, *20*, 987. (c) Duonghong, D.; Ramsden, J.; Grätzel, M. *J. Am. Chem. Soc.* **1982**, *104*, 2977. (d) Moser, J.; Grätzel, M. *Helv. Chim. Acta* **1982**, *65*, 1436. (e) Moser, J.; Grätzel, M. *J. Am. Chem. Soc.* **1983**, *105*, 6547.
(2) (a) Rossetti, R.; Brus, L. *J. Phys. Chem.* **1982**, *86*, 4470. (b) Rossetti, R.; Beck, S. M.; Brus, L. *J. Am. Chem. Soc.* **1982**, *104*, 7321. (c) Fox, M. A.; Lindig, B.; Chen, C. C. *J. Am. Chem. Soc.* **1982**, *104*, 5828. (d) Metcalfe, K.; Hester, R. E. *J. Chem. Soc., Chem. Commun.* **1983**, 133. (e) Chandrasekaran, K.; Thomas, J. K. *Chem. Phys. Lett.* **1983**, *97*, 357. (f) Henglein, A. *Ber. Bunsenges. Phys. Chem.* **1982**, *86*, 301. (g) Brown, G. T.; Darwent, J. R. *J. Phys. Chem.* **1984**, *88*, 4955. (h) Grätzel, M.; Moser, J. *Proc. Natl. Acad. Sci. U.S.A.* **1983**, *80*, 3129.

0002-7863/85/1507-8054$01.50/0